RSC Advances

REVIEW

View Article Online
View Journal | View Issue

Cite this: *RSC Adv.*, 2026, **16**, 16194

Unveiling the rheological secrets of hydrogels: from lab to clinical translation

Jingxin Shan †*[ab] and Weijie Jiao†[c]

Hydrogels have garnered significant attention in the biomedical field due to their high-water absorption capacity, flexibility, and biocompatibility. However, the translation of laboratory achievements related to hydrogels into clinical applications remains slow. Core reasons for this phenomenon lies in the persistent gap between key design elements—such as material selection, manufacturing techniques, and rheological properties—and the practical requirements of clinical applications. Rheology, by investigating the deformation and flow characteristics of hydrogels, provides a critical tool for understanding their mechanical properties and dynamic behaviors. Consequently, the rheological properties of hydrogels serve as a vital "bridge" connecting laboratory research with clinical practice. This study highlights the pivotal role of rheology in the clinical translation of hydrogels. Initially, it analyzes the influence of rheological parameters, including storage modulus, compressive modulus, and viscosity on hydrogel performance, which respectively reflect elasticity, resistance to compression, and flow behavior. Additionally, the article summarizes biomedical applications of hydrogels, such as drug delivery systems, corneal and lens repair, and smart sensors. Future research should focus on the clinical translation of hydrogel rheological properties, ensuring their efficacy, stability, and controllability through systematic studies to meet diverse clinical demands. By integrating advanced biofabrication technologies, the widespread clinical adoption of hydrogels can be further accelerated.

Received 27th November 2025
Accepted 13th March 2026

DOI: 10.1039/d5ra09160h

rsc.li/rsc-advances

1. Introduction

Rheology, as a scientific discipline, is dedicated to elucidating the deformation and flow characteristics of materials when subjected to applied forces.[1,2] Specifically, the alterations in tissue viscoelasticity have become a consensus criterion for early lesions (such as metabolic dysfunction–associated steatotic liver disease,[3] tumor,[4] *etc.*). Meanwhile, shear viscosity has emerged as a biomarker for the detection of chronic kidney disease.[5] The application of rheology within the biomedical field necessitates the interdisciplinary integration of various domains, including physics, chemistry, biology, and materials science. However, in practical research settings, the collaboration among these disciplines is insufficiently robust, and there is a notable absence of effective mechanisms for collaborative innovation. This deficiency has constrained advancements in certain critical technologies and methodologies, thereby impeding the full realization of rheology's potential in biomedical research.[6]

Hydrogels are three-dimensional polymer network structures consisting of polymer chains, wherein hydrophilic polymer moieties undergo hydration driven by thermodynamic forces, resulting in the absorption of substantial quantities of water.[7] These permanent covalent crosslinks restrict the free movement of the polymer chains while still permitting local movement of chain segments to a certain extent.[8] In contrast, reversible links (*e.g.*, supramolecular interactions) can be deliberately designed to relax such constraints and enable significant chain mobility.[9,10] Due to their high-water content, hydrogels exhibit significant flexibility and biomimetic properties.[11–13] Consequently, hydrogels possess exceptional rheological properties, rendering them a focal point in biomedical applications.

Initially, rheological characteristics describe the viscoelastic response of hydrogels under polymer network deformation. Both rheological behavior and mechanical performance/stability are governed by the underlying network structure.[14] By tailoring the crosslinking density (chemically or physically) and specifying the type of molecular weight (polymer chain molecular weight or molecular weight between crosslinks), the storage modulus (linear viscoelastic response under small-amplitude deformations) and mechanical strength (dependent on network heterogeneity and failure modes) of hydrogels can be modulated, respectively. Secondly, the viscoelastic properties of hydrogels could be modulated through the design of

[a]*Department of Biomedical Engineering, He University, No. 66 Sishui Street, Hunnan District, Shenyang, 110163, China. E-mail: shanjingxin@huh.edu.cn; I897708376@163.com*

[b]*School of Intelligent Medicine, China Medical University, No. 77 Puhe Road, Shenyang North New Area, Shenyang, Liaoning Province, 110122, P. R. China*

[c]*Xi'an Jiaotong University, College of Life Science and Technology, Xi'an, China*

† These authors contributed equally to this work.

Table 1 Hydrogels approved for clinical application

Product name	Clinical indications	Core rheological properties	Relationship between rheological mechanisms and clinical outcomes	Ref.
Plenity® (Gelesis)	Weight management: used to enhance satiety and assist in controlling dietary intake	A solid gel structure that forms and maintains a high elastic modulus (G') under the low-shear environment of the stomach	Within the stomach, the gel forms numerous units exhibiting mechanical strength and hardness comparable to those of food. Its high G' value ensures that the gel occupies volume effectively and resists deformation induced by gastric peristalsis, thereby triggering satiety through physical filling	20 and 21
ReSure® Sealant (ocular Therapeutix)	Ophthalmic surgery: used post-cataract surgery to seal clear corneal incisions and prevent aqueous humor leakage	The storage modulus (G') reaches a peak within a short time; the material exhibits a loss modulus (G'') and adhesive force, and the moduli decrease in a time-controllable manner	Rapid gelation (a rapid increase in G') enables clinicians to achieve immediate and precise intraoperative wound closure, forming a physical barrier. Appropriate viscoelasticity (a balance between G' and G'') ensures that the gel conforms to irregular wound surfaces and resists shear forces induced by blinking	22 and 23
Embrace™ HES (Instylla)	Vascular intervention: a liquid embolization system for occluding peripheral hypervascular tumors	Prior to injection it behaves as a low-viscosity Newtonian fluid; upon co-injection rapid crosslinking occurs, the elastic modulus (G') increases, and a solid-like gel is formed	Ultra-low viscosity ensures that the two precursor liquids can easily traverse microcatheters and penetrate deeply into the terminal microvasculature of tumors. A rapid liquid-to-solid transition (a sudden increase in G') enables the gel to form *in situ* within target vessels instantaneously, fully filling the lumen and achieving immediate, complete occlusion of blood flow	24

crosslinking dynamics and engineering of network topology. Viscoelastic behavior arises from the combined elastic response of polymer networks and time-dependent viscous dissipation associated with chain mobility, bond dynamics, and solvent–polymer interactions.[15] It is also possible to reducing the polymer molecular weight decreases chain entanglement and thus accelerates stress relaxation,[16] whereas employing ultra-high-molecular-weight polymers can produce topologically entangled "knotted" colloids that serve as highly elastic scaffolds.[17] Lastly, viscoelasticity of hydrogel not only provides physical support but also functions as a dynamic mechanical signal that cells sense and transduce into biochemical responses. Viscoelastic hydrogels with high loss modulus significantly promote the expression of osteogenic and chondrogenic genes in BMSCs, facilitating the proliferation and spreading of bone marrow mesenchymal stem cells,[18] and hydrogels with rapid stress-relaxation characteristics effectively recruit endogenous neural stem cells to migrate to injury sites, thereby supporting neural functional recovery.[19]

Currently, several hydrogel products with have been approved for clinical applications (Table 1). *E.g.*, Plenity® (Gelesis) was applied to weight management due to solid gel structure that forms and maintains a high elastic modulus under the low-shear environment of the stomach.[20,21] ReSure® Sealant (Ocular Therapeutix) was used in ophthalmic surgery because of the storage modulus (G') and loss modulus (G'') can rapidly elevate at the ocular site to undergo *in situ* solidification.[22,23] Moreover, Embrace™ HES (Instylla) was applied in vascular intervention due to upon co-injection rapid crosslinking occurs and a solid-like gel is formed.[24]

Table 2 Summary of hydrogel rheological characterization methods

Test method	Core test parameters	Physical significance	Application-oriented insights	Reference
Stress relaxation	Relaxation time (τ), residual stress ratio	τ reflects bond recombination rate; residual stress ratio indicates irreversible plastic deformation	Predicts long-term stability post-implantation (*e.g.*, anti-adhesion barriers)	16, 39 and 40
Creep test	Steady-state creep rate, recovery rate (%)	Reflects molecular chain slippage or elastic recovery: high recovery rate (>80%) indicates elasticity dominance	Optimizes anti-collapse tailored mechanical properties and scaffolds	41–44
Oscillatory shear	Storage modulus (G'), loss modulus (G''), loss tangent (tan δ)	G'/G'' ratio determines solid/liquid state ($G'>G''$ means gel status); tan $\delta = G''/G'$ quantifies energy dissipation	Filters 3D bioinks (*e.g.*, G' > 2500 Pa & tan δ < 0.2 ensure shape retention)	45 and 46

In this study, we commenced by investigating the rheological properties of hydrogels. Following this, we delineated a range of applications for hydrogels within the biomedical field, such as drug delivery systems, corneal and lens repair, and smart sensor technologies. Finally, we provided innovative insights into the potential developmental pathways for hydrogels in the biomedical sector. We suggest that the integration of rheological properties with insights gained from successful translational experiences in other hydrogel applications constitutes a promising approach to advancing the clinical translation of hydrogels.

2. Rheological characteristics of hydrogels

2.1 Definition of rheological characteristics for hydrogel

Rheological properties of hydrogels can be broadly categorized into viscosity and modulus, both of which are intrinsic physical attributes of the material.[25] Viscosity refers to the internal frictional resistance encountered by the fluid during flow.[26] At a specified rotational shear rate, the apparent shear viscosity is quantified as the ratio of shear stress to shear rate. Typically, the viscosity of the hydrogel is measured under controlled conditions of time and temperature, in a specified direction (or at a particular angular frequency), and at a regulated shear rate.[27,28]

Modulus of a material is defined as the ratio of stress to strain when the material is subjected to stress. The term "modulus" encompasses various types, including tensile modulus,[29] compression modulus,[30] shear modulus[31] and torsional modulus.[32] Theoretically, the equivalence between tensile and compressive modulus, as well as between shear and torsional modulus, strictly holds only for linear, isotropic, elastic materials under small deformations. Soft hydrogels, whereas, typically exhibit pronounced viscoelasticity, nonlinearity, and time – dependent behavior, which cause significant deviations from these idealized assumptions. Concurrently,

Table 3 Hydrogel properties evaluated through rheology testing methods

Hydrogel properties	Rheological testing procedures	Characterization of hydrogel properties	Key parameters and reference
Shear thinning	Shear measurement	Manifested by a decrease in viscosity with increasing shear rate	Hydrogels exhibit shear-thinning behavior (a critical property for extrusion-based 3D printing)[47]
Self-healing	Oscillatory time sweep	By periodically applying high and low strains, the process of material damage and subsequent repair is simulated	Rapid recovery of G' indicates network reconstruction[48]
Photosensitivity	Oscillatory time sweep (with concurrent light irradiation at specific wavelengths)	Simultaneously activating or deactivating light sources of specific wavelengths while monitoring the temporal evolution of the storage modulus G'	Under illumination the storage modulus (G') increases, and gelation occurs.[49]
Thermosensitivity	Dynamic temperature ramp	Change the temperature and monitoring variations in G' and G''. The abrupt changes in G' and G'' signaling a sol–gel/gel–sol phase transition	Correlation with material's thermosensitive swelling behavior.[50]

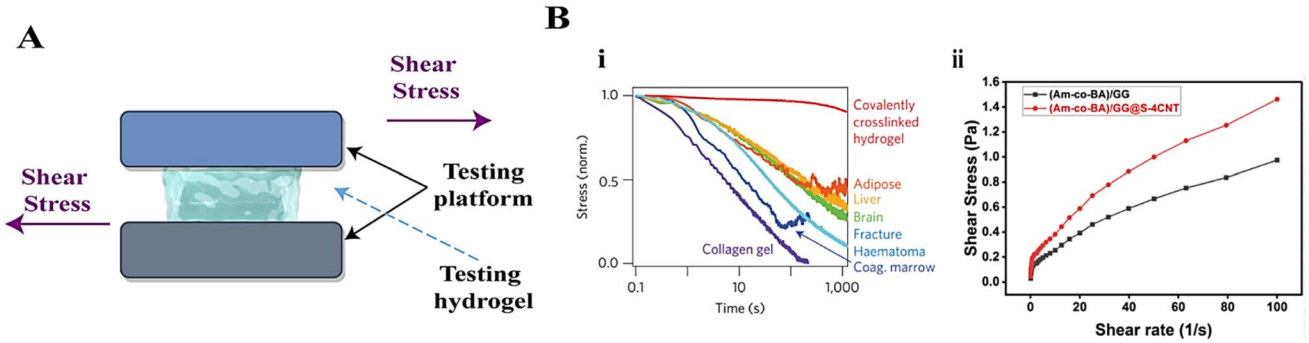

Fig. 1 (A) Schematic of a stress-relaxation test. Hydrogel was emplaced between two impermeable rigid plates, and a strain is suddenly applied to the hydrogel. The figure was draw by Figdraw. (B) (i) Stress relaxation tests of a collagen gel and other tissue. Adapted with permission from Nature Portfolio,[16] copyright 2016. (ii) Stress relaxation tests of hydrogels composed of two different components. The intersection of the red and black curves indicates the formation of hydrogen bonds. Adapted with permission from Elsevier,[51] copyright 2025.

rheological characterization of hydrogels is predominantly based on shear deformations, while tensile/compressive and shear/torsional modulus constitute commonly used metrics for describing deformation performance in hydrogel studies.

Rheological properties of hydrogels are primarily characterized by the loss modulus and storage modulus.[33] The loss modulus (G''), also known as the viscous modulus, measures the energy dissipated due to viscous (irreversible) deformation, thus reflecting the material's viscosity. Conversely, the storage modulus (G'), also referred to as the elastic modulus, quantifies the energy stored in a material as a result of elastic deformation, thereby indicating the material's elasticity. The ratio of the loss modulus (G'') to the storage modulus (G'), denoted as $\tan\delta = G''/G'$, is referred to as the loss tangent.[34] It serves as a fundamental concept in rheology, quantifying the proportion of energy dissipation to energy storage in materials subjected to cyclic deformation. The variation in the loss tangent can reflect changes in the internal structure of hydrogels, particularly

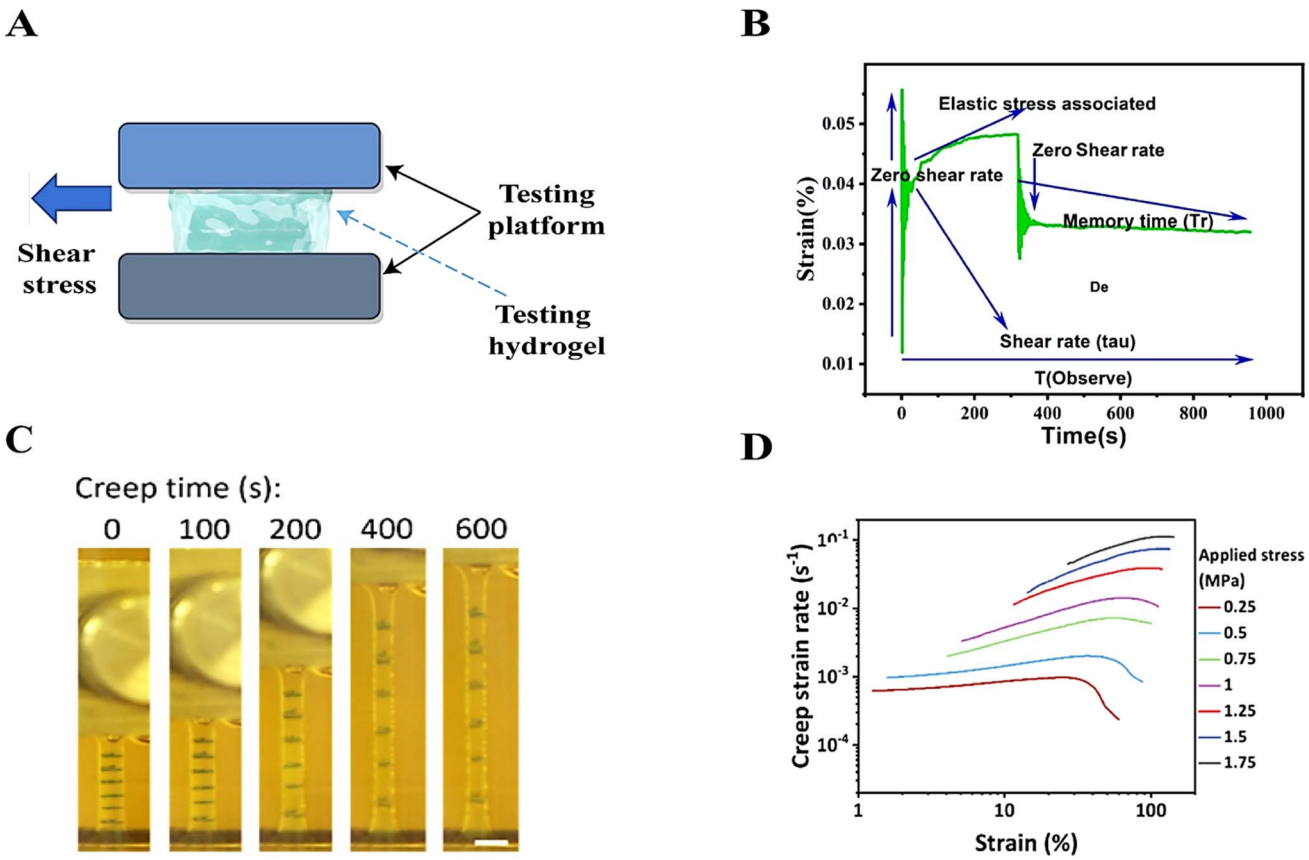

Fig. 2 (A) Schem of creep testing procedure. This figure was drawn by Figdraw. (B) Strain as a function of time during creep recovery test. Adapted with permission from Elsevier,[44] copyright 2025. (C) Hydrogel with different creep times under 0.5 Mpa. Scale bar = 5 mm. (D) Creep strain rate with respect to creep strain at various applied stress. Adapted with permission from ACS publications,[52] copyright 2025.

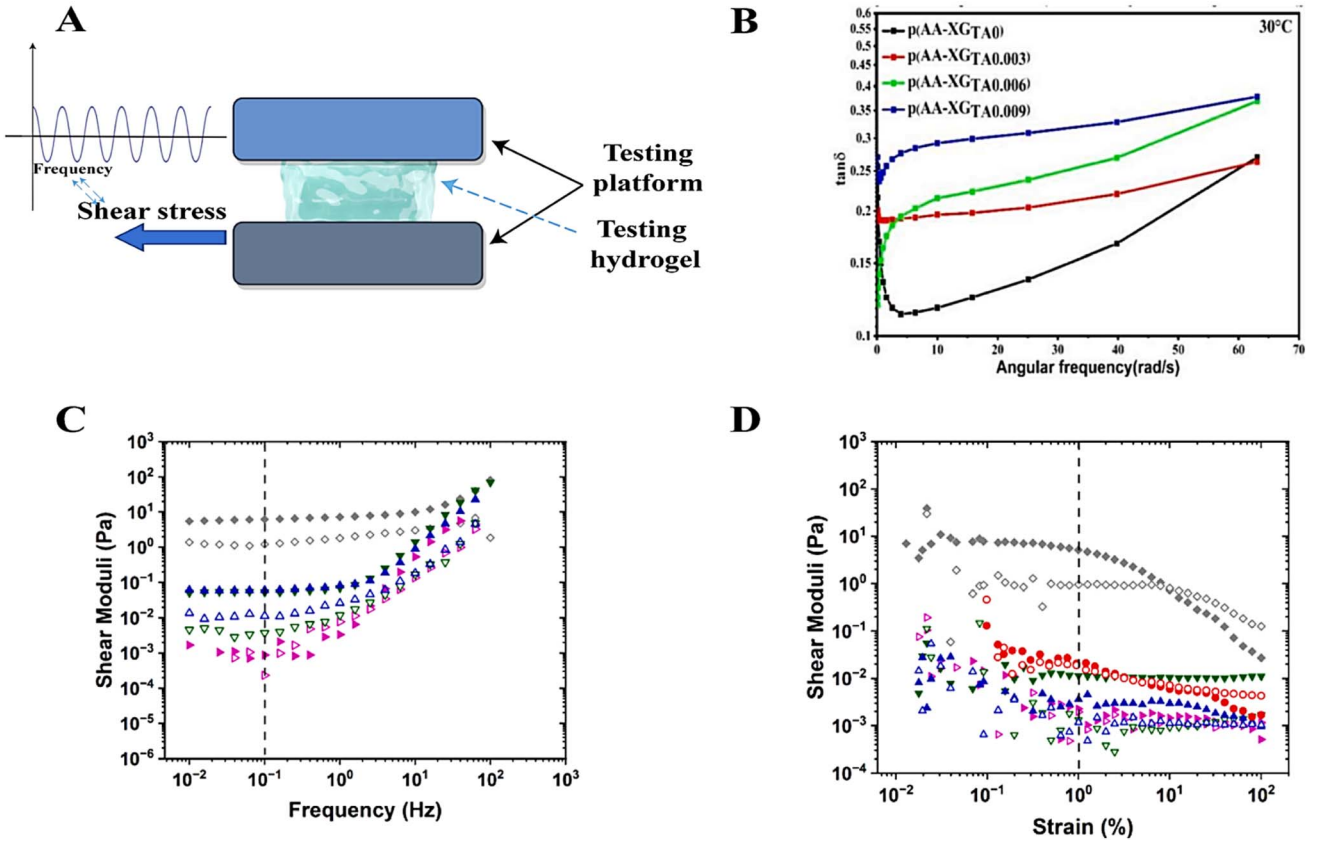

Fig. 3 (A) Schem of oscillatory shear testing procedure. This figure was drawn by Figdraw. (B) The influence of different components on the oscillatory shear properties of polymers (indirectly reflecting the viscoelastic characteristics of polymers with varying components). Adapted with permission from Elsevier,[54] copyright 2025. (C) Small-angle oscillatory shear measurements with varying frequency at a strain of 1% and (D) strain at a frequency of 0.1 Hz across four decades of values. Adapted with permission from Elsevier,[45] copyright 2024.

during the sol–gel transition, where this characteristic becomes especially pronounced.[35]

2.2 The significance of rheological parameters for hydrogels

Rheology specifically characterizes a material's viscoelastic response under shear deformation, where key parameters (storage modulus G', loss modulus G'', dynamic viscosity η, *etc.*) exhibit time-and frequency dependent viscoelastic behavior. These parameters reflect the balance between elasticity and viscosity, as well as the dynamic response of the internal structure (such as network relaxation and crosslinking density).

Among rheological descriptors, the storage modulus (G') is of great importance. It measures a hydrogel's ability to store elastic energy during shear deformation, and is directly related to its elastic recovery behavior. A higher G' indicates a stronger elastic response and better resilience to cyclic mechanical loading.[36] This time – frequency viscoelasticity ensures that the hydrogel can maintain structural stability under dynamic mechanical stimuli, which is a crucial feature for applications that require repeated deformation.

In contrast, the compression modulus, measured through quasi- static compression tests, describes a hydrogel's resistance to axial compressive deformation. Although the testing method of the compression modulus is different from rheological shear analysis, rheological parameters like G' can provide microscopic insights into the network stiffness (such as crosslinking density and chain entanglement), which underlie macroscopic mechanical behaviors. For instance, hydrogels with a high G' often have a higher compression modulus because of a more robust internal network. This is very important for applications such as cell encapsulation or creating cellular microenvironments.[37,38]

2.3 Experiment methods for rheological characteristics of hydrogel

As a window for observing the internal structure of materials, rheological properties play an important role in the research of hydrogels. The rheological properties of hydrogels can be characterized through experiments such as stress relaxation, creep testing, and oscillatory shear. The differences and significance of testing various rheological properties are briefly summarized in Table 2. Moreover, hydrogel properties (self-healing, shear-thinning, photo/thermo- responsiveness) that could be evaluated using rheology testing methods. The detail information is summarized in Table 3.

2.3.1 Stress relaxation. Stress relaxation arises from the time-dependent reorganization of the internal network structure, such as polymer chain rearrangement, bond exchange, or

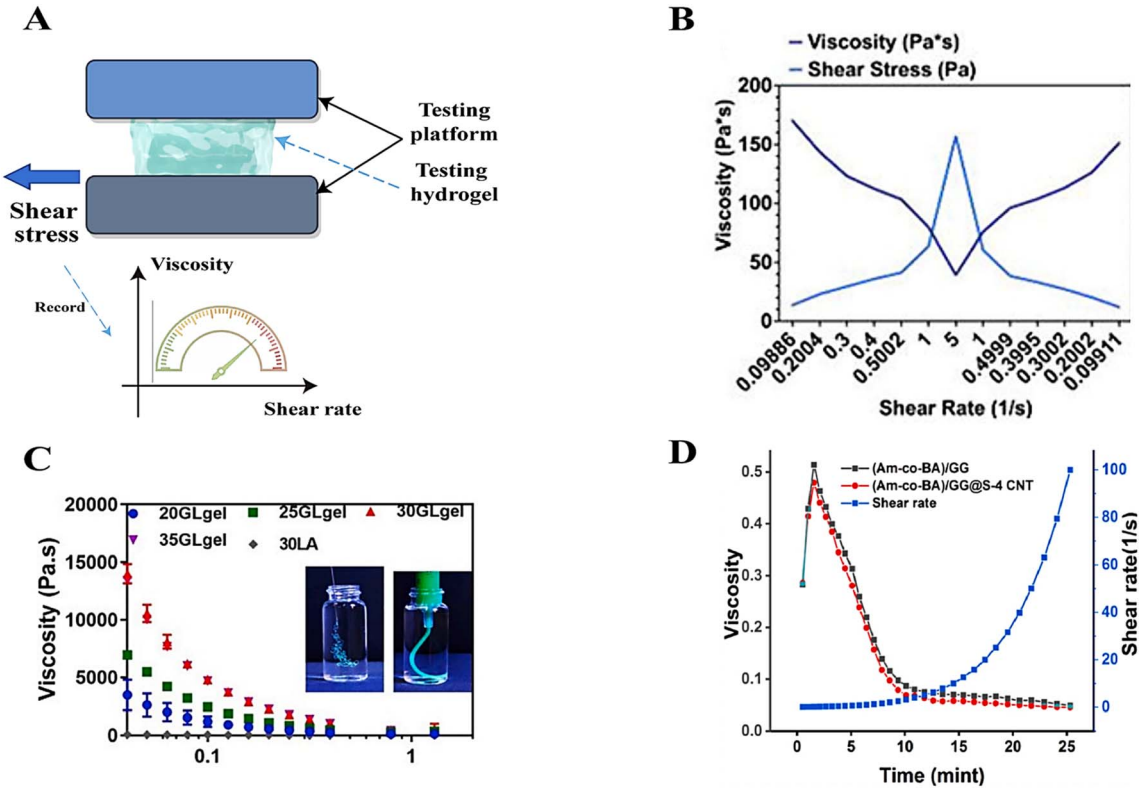

Fig. 4 (A) Schem of shear thinning testing. Powered by Figdraw. (B) Rheological characterization of shear-thinning nanoparticle/hyaluronic acid hydrogel formulations. Adapted with permission from Wiley-VCH GmbH,[56] copyright 2023. (C) Shear rate sweep of glycosaminoglycan nanoparticles coupling LAPONITE® (GLgels) with different compositions with macroscopic images of the GLgel. Adapted with permission from Elsevier,[55] copyright 2021. (D) Reversible shear thinning behavior of the hydrogel for 3D printing. Adapted with permission from Elsevier,[51] copyright 2025.

fluid redistribution in response to an imposed deformation, rather than from deformation alone. During stress relaxation testing, hydrogel sample was placed in a rheometer, subjected to an instantaneous step strain, and recorded shear deformation.[16] Normally, the time-dependent decay curve of the shear stress was measured, thereby obtaining the stress relaxation characteristics. Fig. 1A illustrate the testing progress. Biological tissues exhibit time-dependent decay of internal stress when subjected to external strain, which is critical for dispersing mechanical loads and accommodating deformation.[39] Tissues can actively adapt to changes in mechanical environment through cellular processes such as extracellular matrix secretion and network remodeling. In contrast, the relaxation behavior of hydrogels is largely fixed once the network is formed, unless the network chemistry is specifically engineered to respond to environmental stimuli (Fig. 1B). Therefore, replicating biological stress-relaxation behavior requires the incorporation of controllable, reversible interactions and precise tuning of their kinetics so that the material network acquires dynamic dissipative properties analogous to those of biological tissues.[40,51]

2.3.2 Creep test. Creep test can evaluate the deformation recovery capability of hydrogels under prolonged load. The specific testing procedure involves mounting the hydrogel sample on a rheometer, applying a constant shear stress to the sample, and recording the variation in strain over time.[41] Fig. 2A manifested the testing procedure. An elastic stress associated range within the creep test where material shear stress increases with increase in the shear rate till the flow point from yield point within the yield zone (Fig. 2B).[44] Creep behavior of hydrogels is influenced by their chemical composition and crosslinking density, which can be precisely controlled by adjusting the type and ratio of crosslinking agents (Fig. 2C and D).[42] In practice, creep testing provides insights into the elastic stress associated range within the creep test,[44] and long-term deformation behavior and flow characteristics of hydrogels,[43] both of them playing a critical role in the development of clinical hydrogel products with tailored mechanical properties.

2.3.3 Oscillatory shear. Oscillatory shear testing primarily reveals the viscoelastic and structural responses of hydrogels. The testing procedure, as shown in Fig. 3A. Oscillatory shear involves placing the hydrogel sample into the rheometer's testing fixture, applying periodic oscillatory shear forces, and measuring the variations in its storage modulus and loss modulus over time (Fig. 3B), frequency (Fig. 3C), or strain amplitude (Fig. 3D).[45] Oscillatory shear performance reflects the network fracture threshold and dynamic bond reorganization capability, which are closely associated with the internal network structure (*e.g.*, hydrogen bonds) of hydrogels and external solvents,[46] and serves as a critical evaluation metric for

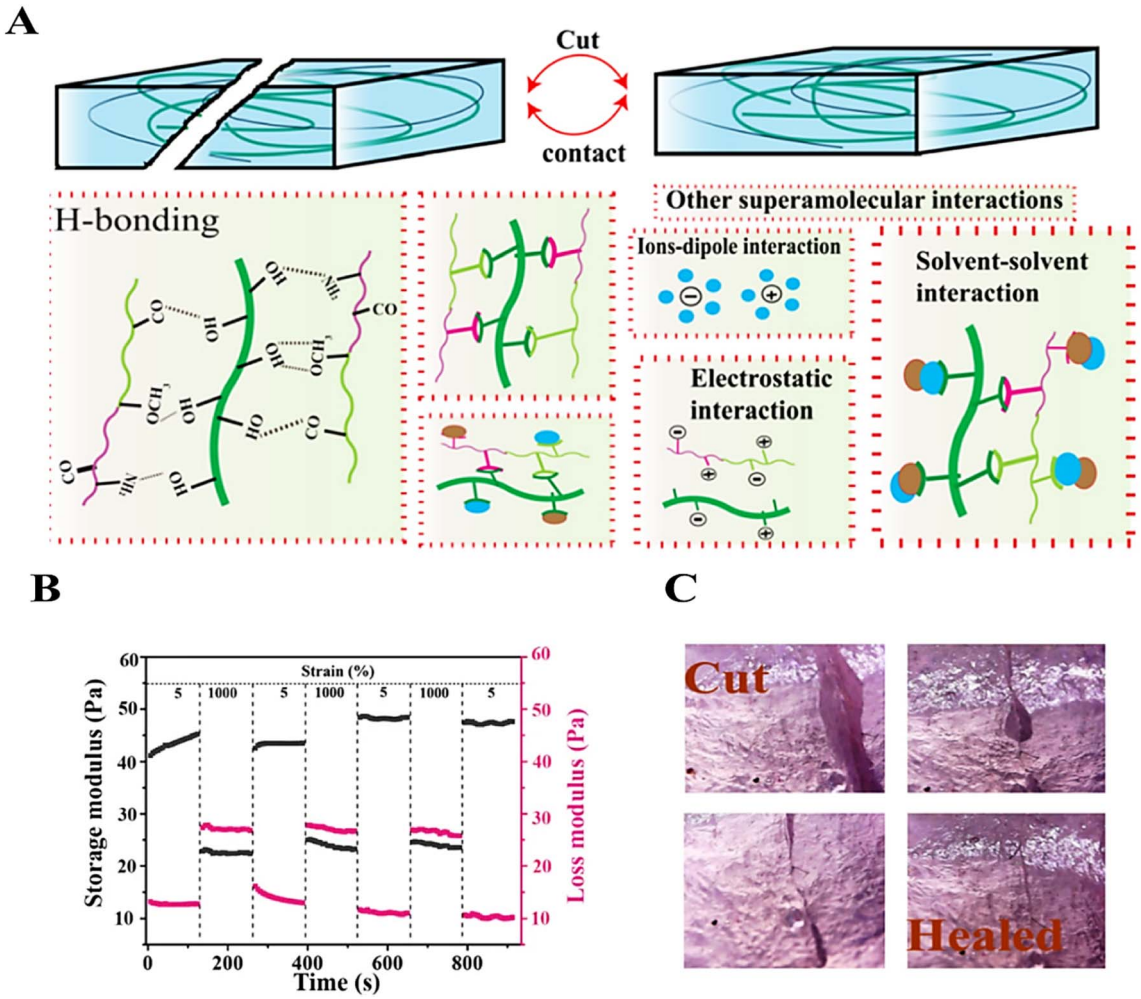

Fig. 5 (A) Schema of self-healing mechanism. Adapted with permission from Royal Society of Chemistry,[61] copyright 2025. (B) Self-healing capacity of the hydrogel. Scale bar = 1 cm. Adapted with permission from Wiley-VCH GmbH,[60] copyright 2022. (C) Digital photographs of the healing gel. Adapted with permission from Royal Society of Chemistry,[61] copyright 2025.

clinically applicable products such as injectable and self-healing materials.[53]

2.3.4 Shear thinning. Shear thinning in hydrogels corresponds to a decrease in viscosity with increasing shear rate due to reversible changes in the polymer network or crosslinking interactions, rather than solely particle-level effects.[55] This procedure involves incrementally increasing the shear rate or shear strain in a specified direction and assessing its impact on viscosity. Fig. 4A specifies the process of shear thinning. A gradual decrease in viscosity or modulus with increasing shear

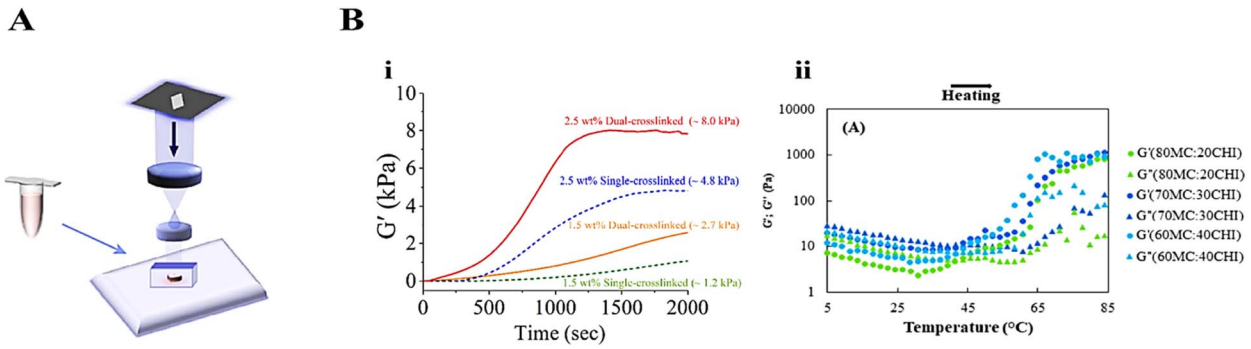

Fig. 6 (A) Schem of photosensitive. Adapted with permission from Elsevier,[62] copyright 2024. (B) (i) Storage modulus (G') of photo-dimerized anth-chitosan-MA hydrogels were measured for 1.5 and 2.5 wt%, respectively within 2000 s. Adapted with permission from Elsevier,[49] copyright 2021. (ii) Storage (G') and loss (G'') modulus for MC: CHI hydrogels at heating. Adapted with permission from Elsevier,[50] copyright 2022.

Table 4 Summary of representative rheological hydrogel with biomedical application

Categories	Hydrogel constituent materials	Rheological properties	Specifical rheological parameter	Application prospective	Ref.
Drug delivery	(PLGA-PEG-PLGA)/Cmab/PCZ	"Sol to gel" status transition	Storage modulus (G') and loss modulus (G'')	Promoted NK cell infiltration into tumor tissues	67
	PVA	Swelling in tissue fluid	Swelling ratio in simulated wound tissue	Wound dressing shown more blood compatibility	68
	Gelatin microspheres@ PDA @ Lipo-Ebselen	Excellent adhesive properties at middle ear cavity	Adhesiveness	A strong ability of hearing recovery	69
	PACAP/PEG	Deformation and recovery	Linear viscoelastic region and step-strain measurements	Maintaining retinal integrity and suppressing apoptosis	70
Corneal and eye repair	pDCSM, HAMA	Gelled at the beginning and formed into hydrogel after exposed to light	Prior to illumination, the hydrogel exists in a flow-dominated rheological state (storage modulus $G' <$ loss modulus G'')	Hydrogel adhered to the stroma bed with long-term retention	71
	Alginate-capped nanoceria (Ce-Alg)	Viscosities	Viscosities reduced upon increasing the shear velocity	Maximum grafting amount of alginate reduced epithelial injury area by ~99%	72
	Heparin-gelatin	Tunable mechanical strength	Moduli, swelling ratio, storage modulus (G')	Limited the influx of inflammatory and fibrotic cytokines	73
	DNA supramolecular hydrogel	Strong mechanical strength, shear-thinning behavior and rapid recoverability	Moduli, storage modulus (G') and loss modulus (G'')	Morphology and basic functions of the operated eyes are well recovered	74
	Tetra-armed PEG	Appeared as transparent soft jelly and exhibited storage modulus stably kept at ~10 Pa	Storage modulus (G'), loss modulus (G'') and swelling ratio	Achieve a synergistic antitumor effect to inhibit tumor recurrence	75
	Polycarboxybetaine and dithiothreitol	A stable rheological property at a high frequency	Storage modulus (G') and loss modulus (G'')	Rapidly formed hydrogel in rabbit eyes vitreous cavity and remains stable	76
	Two peptide hydrogels (3K-OX: positive charges. 3E-OX: negative charges)	Shear-thin recovery and self-assemble properties	Storage modulus (G') and loss modulus (G'')	Closely resembles the structure and functions of the native vitreous body	77
Flexible and smart sensor	PVA/ALG/cellulose nanofibers/ sodium tetraborate	Viscosity decreases gradually as the shear rate increases	Storage modulus (G'), loss modulus (G''), viscosity with shear rate	Monitor human movements in real time	78
	Poly(acrylamide)	A stable adhesion and stretchability	Velocity	Unusual features of high mass-permeability and low impedance	79
	PVA, PA, gelatin	Possesses good temperature–responsive viscosity	Shear thinning, storage modulus (G')	Can be recycled based on their reversible physical bonding	80
	Adhesive and hydrophobic bilayer hydrogel	Excellent viscosity, twist and compress	Adhesiveness and velocity	A portable headband for EEG-based emotion classification	81

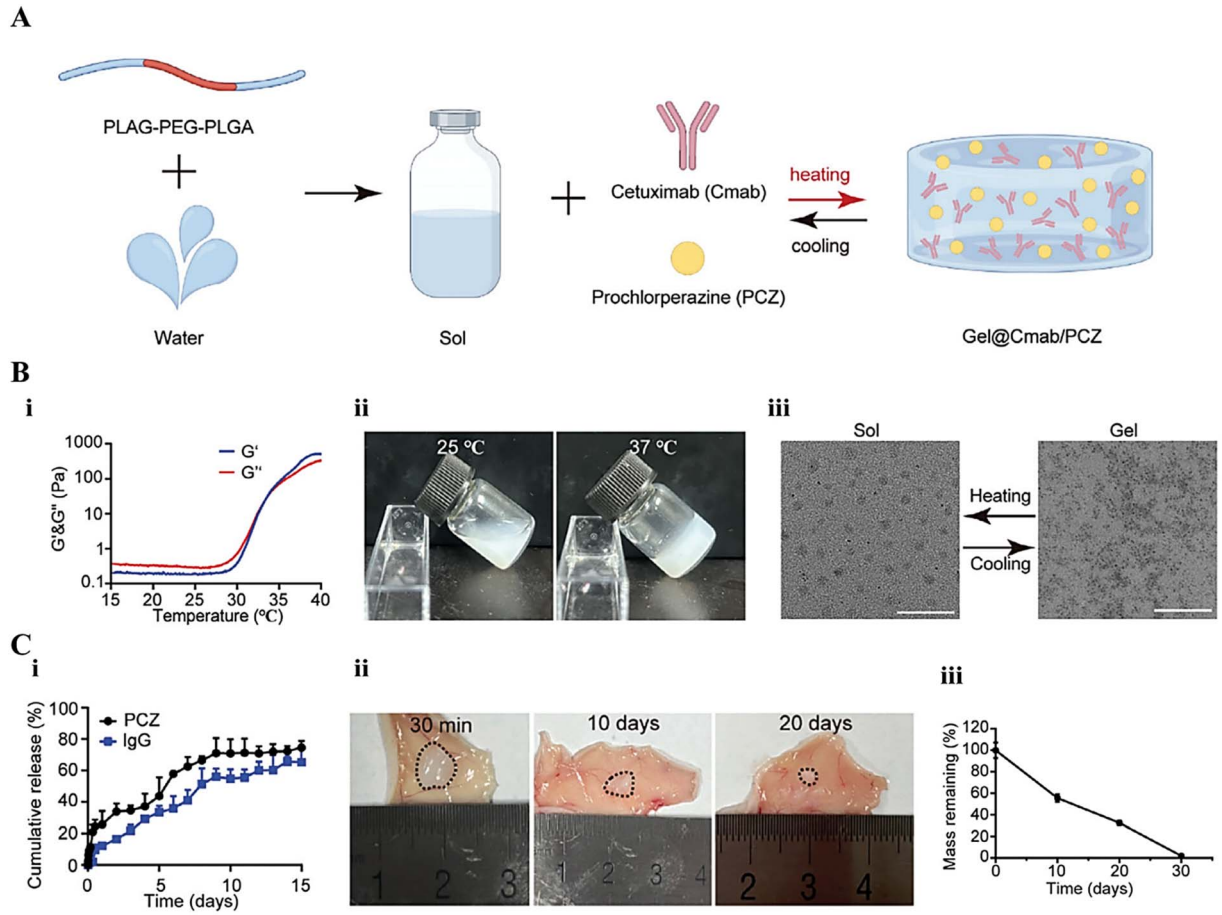

Fig. 7 (A) Schematic illustration of the preparation of Gel@Cmab/PCZ. (B) (i) The storage modulus (G') and loss (G'') modulus of gel. (ii) Photographs of the sol-to-gel transition with the increasing temperature. (iii) Representative TEM images of thermo-sensitive sol–gel translation (10 wt%). (C) (i) Cumulative release profiles of PCZ and Cmab from hydrogels incubated with PBS at pH 7.4 ($n = 3$). (ii) Representative photographs of gel at different time points after subcutaneous injection in mice. (iii) Quantitative analysis for gel's degradation. Adapted with permission from Wiley-VCH GmbH,[67] copyright 2024.

rate or shear strain indicates that the hydrogel under investigation exhibits shear thinning properties (Fig. 4B and C).[55,56] The variation of viscosity relative to yield stress can be used to indirectly assess changes in the chemical bonds within the hydrogel. A decrease in viscosity following its surpassing the yield stress indicates the rupture of hydrogen bonds inside the hydrogel (Fig. 4D).[51] Shear thinning endows hydrogels with excellent fluidity and processability during, making it a crucial performance parameter that must be evaluated for clinical products like "injectable formulations" and "dressings".[57]

2.3.5 Self-healing. The reparative capability of self-healing hydrogels originates from their internally constructed networks of dynamic reversible bonds. Their healing mechanisms are primarily divided into chemical repair mechanisms (where covalent bonds break at damage sites but can reform under specific conditions) and physical repair mechanisms (where noncovalent interactions rupture under applied force and rapidly reassemble once the force is removed),[58] respectively. Fig. 5A illustrates the specific self-healing mechanism. In practical applications, oscillatory shear time-sweep testing can be employed to characterize self-healing behavior.[59] Typically, a large-amplitude oscillatory shear is first applied to disrupt the gel network (resulting in a decrease in the storage modulus G' or a drop below the loss modulus G'', such that the material behaves as a fluid). Thereafter, the deformation is switched to small-amplitude oscillatory shear and the temporal evolution of G' and G'' is monitored. If the moduli recover to values comparable to those at small strain, this indicates that the hydrogel possesses self-healing capability (Fig. 5B and C).[60]

2.3.6 Photosensitivity or thermosensitive. The photosensitive properties of hydrogels originate from the reversible structural changes of photoresponsive moieties (chromophores) introduced into the material upon absorption of light at specific wavelengths, while thermosensitivity is typically related to temperature-dependent changes in the hydrophilic–hydrophobic balance of the polymer chains.[62] Fig. 6A specifies the process of photosensitivity and thermosensitive. For photocurable gels, the process in which G' increases from zero or a low value upon illumination and ultimately reaches a plateau reflects the kinetics of the photochemical crosslinking reaction, as shown in Fig. 6B i.[49] For thermosensitive hydrogels, the temperature at which G' exhibits a sudden increase during

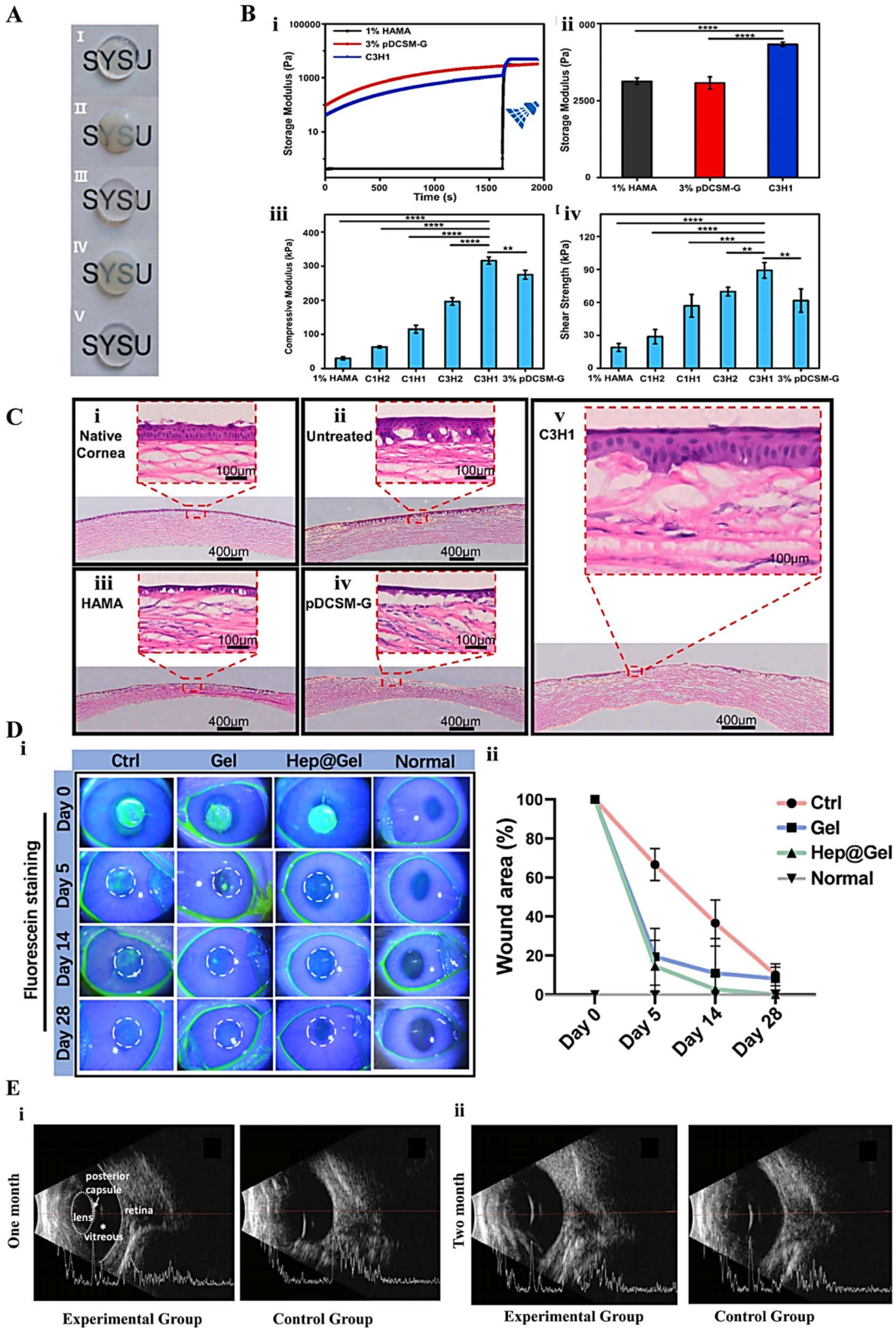

Fig. 8 (A) (i) Photocrosslinked HAMA. (ii) Physically crosslinked pDCSM-G without CMC/NHS. (iii) CMC/NHS crosslinked pDCSM-G. (iv) Photocrosslinked C3H1 hybrid hydrogel without CMC/NHS. (v) Dual-crosslinked C3H1 hydrogel. (B) (i) Rheological characterization of the photocrosslinked 1% HAMA, CMC/NHS crosslinked pDCSM-G, and dual-crosslinked C3H1 hydrogel. (ii) Storage modulus of the HAMA, pDCSM-G, and C3H1 hydrogels. (iii) (iv) Compressive modulus and shear strength of the hydrogels with different compositions of HAMA and pDCSM-G, respectively. (C) Histological analysis of the hydrogel treated rabbit corneas eight weeks post-operation. (i) Native corneas without defect. (ii) Corneas with untreated defect, and the defected corneas filled with (iii) HAMA hydrogel, (iv) pDCSM-G, and (v) C3H1 hydrogel. Adapted with permission from Elsevier,[71] copyright 2023. (D) (i) Evaluation of corneal wound healing by fluorescein staining. The green area indicated the

heating can be regarded as the gel phase transition temperature, as shown in Fig. 6B ii.[50] The photo/thermal responsiveness enables hydrogels to alter their structure and properties under illumination, thereby achieving responsiveness to external stimuli, which constitutes a crucial characteristic in applications of smart materials and sensors.[63]

3. Rheological hydrogel applied in biomedical area

The rheological characteristics of hydrogels are crucial in biomedical applications due to their mechanical properties and biocompatibility, rendering them optimal materials for tissue engineering, drug delivery, and biosensor applications. Rheological analysis offers quantitative insights into the assembly of hydrogel networks.[64] Furthermore, these properties significantly influence the behavior of hydrogels during injection and implantation processes. Specifically, in the case of injectable hydrogels, rheological properties dictate their fluidity and stability *in vivo*.[65] Moreover, the rheological properties of hydrogels can be augmented through the incorporation of dual network structures or nanocomposites, thereby enhancing their mechanical properties and functionality.[14,66] The main application of rheological hydrogel was summarized in Table 4.

3.1 Drug delivery

The three-dimensional network structure of hydrogels facilitates the encapsulation and protection of drug molecules, thereby preventing their degradation or inactivation during delivery and ensuring their effective release upon reaching the target site.[82–84] By modulating the cross-linking density and structure of the hydrogel, it is possible to design smart hydrogels that release drugs under specific conditions.[85,86] In drug delivery, the rheological properties determine the injectability of hydrogels and the performance of drug release. In this context, the rheological properties, such as viscosity and modulus, are the primary parameters influencing the rate and duration of drug release.[87,88]

Wu, C., *et al.* constructed an injectable thermoresponsive hydrogel (Gel@Cmab/PCZ) to codeliver cetuximab (Cmab) and prochlorperazine (PCZ) for colorectal cancer treatment.[67] The gel was made through PLGA-PEG-PLGA and can transition from *via* ring-opening polymerization (Fig. 7A). Rheological testing shows that the storage modulus (G') and loss modulus (G'') remain consistently low and stable from 15 °C to 30 °C, suggesting that the material behaves more fluidly within this temperature range. As the temperature approaches 30 °C, G' and G'' begin to increase sharply, with the rate of increase for G' surpassing that of G''. This behavior is indicative of a gelation or cross-linking reaction within the hydrogel, resulting in a more solid and elastic structure, characteristic of a "sol–gel" transition (Fig. 7B i). Upon heating the PLGA-PEG-PLGA gel solution to 37 °C for 2 min, a sol-to-gel transition occurred, resulting in a stable, milky white hydrogel named Gel@Cmab/PCZ (Fig. 7B ii, iii). Besides, this hydrogel can serve as a sustained release reservoir for the active ingredients PCZ and Cmab (Fig. 7C i). Meanwhile, a white hydrogel formed within 30 min post-injection and gradually degraded over time (Fig. 7C ii, iii).

Additionally, an innovative hydrogel, polyvinyl alcohol (PVA), has been identified as a promising candidate for mucoadhesive and drug delivery applications. Singh *et al.* discovered PVA hydrogel crosslinked with sterculia gum exhibited strong adhesive strength with the mucous membrane.[68] This finding indicates that PVA hydrogel films could effectively adhere to wound sites, providing a protective barrier against pathogens and positioning them as viable candidates for drug delivery systems. Furthermore, Chen *et al.* grafted polydopamine (PDA) onto the surface gelatin microspheres (GM) and loaded drug ebselen liposomes (Lipo-ebselen) to develop a drug-releasing hydrogel GM@PDA@Lipo.[69] The GM@PDA hydrogel could firmly adhere to the round window membrane, which provided conditions for the hydrogel to release drugs at a fixed point and prolonged the release time. Chen, M., *et al.* developed pituitary adenylate cyclase-activating polypeptide (PACAP)/PEG hydrogel to promote the recovery of retinal function.[70] The linear viscoelastic region for Gel-PEG and PACAP@Gel-PEG hydrogels was 9.9% and 6.3%, respectively, indicating both hydrogels can withstand relatively large deformations without being destroyed. In the step-strain measurements, when the strain was switched from a high magnitude strain (1000%) to a low magnitude strain (1%), both Gel-PEG and PACAP@Gel-PEG hydrogels recovered completely in a few seconds, showing both hydrogels having good structural recovery ability. Such rheological properties indicated that hydrogel has good fluidity and structural recovery ability and can reduce cell apoptosis and microglial activation in the retina. This shows that it has a good therapeutic effect on retinal ischemia.

3.2 Corneal and eye repair

The rheological properties of hydrogels facilitate the emulation of the mechanical attributes and structural features of the natural ECM, thereby providing an optimal environment for cellular growth.[62,89] Furthermore, these rheological properties significantly influence the interactions between hydrogels and biological cells and tissues. Concurrently, suitable rheological characteristics enhance the integration of hydrogels with adjacent tissues, thereby promoting tissue regeneration and functional recovery.[90] Meanwhile, the rheological properties influence the regulation of cellular behavior by hydrogels and their own stability *in vivo*. In the context of corneal and ocular repair, hydrogels are required to exhibit high optical transparency, appropriate mechanical strength, and self-healing capabilities.[91,92]

Shen, X., *et al.* utilized porcine decellularized corneal stroma matrix (pDCSM) and methacrylated hyaluronic acid (HAMA)

epithelial defects. (ii) Quantification of corneal wound healing. Adapted with permission from Creative Commons Attribution License 4.0 (CC BY),[73] copyright 2024. (E) (i) (ii) Ultrasound images of the retina and intraocular lens at 1 month and 2 months after surgery, respectively. Adapted with permission from Wiley,[74] copyright 2021.

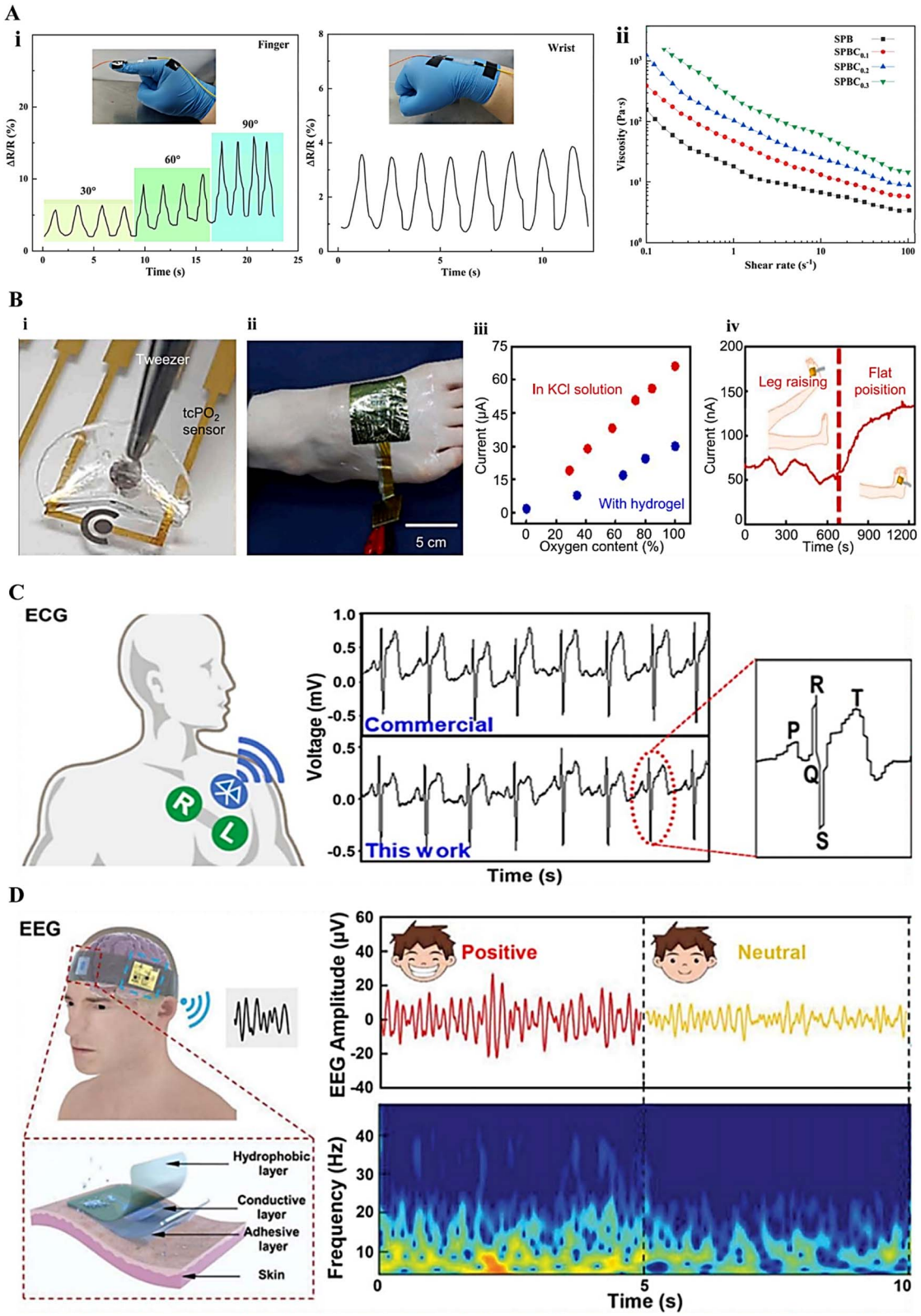

Fig. 9 (A) (i) SPBC hydrogels were used as monitoring sensors for finger and wrist electrical experiments, respectively. (ii) The shear rate table for SPBC hydrogels. Adapted with permission from Creative Commons Attribution (CC BY),[78] copyright 2024. (B) (i) Image of a $tcPO_2$ sensor composed of a hydrogel and a three-electrode electrochemical device. (ii) Image of a $tcPO_2$ sensor mounted on the foot using a flexible medical-grade substrate. (iii) Linear correlation between oxygen concentration and reduction current measured by a $tcPO_2$ sensor with a liquid electrolyte and hydrogel interface. (iv) *In vivo* $tcPO_2$ measurements under various leg positions. Adapted with permission from Commons Attribution Non-Commercial License 4.0 (CC BY-NC),[79] copyright 2021. (C) An electrocardiogram electrode scheme. Adapt with permission from Nature Portfolio,[80] copyright 2022. (D) An electroencephalogram electrode scheme. Adapted with permission from Wiley-VCH GmbH,[81] copyright 2022.

together to address tissue regeneration after corneal defect.[71] Both chemically crosslinked hydrogels, including the photo-crosslinked HAMA, CMC/NHS crosslinked pDCSMG, and the dual-crosslinked hybrid hydrogel, exhibited excellent transparency (Fig. 8A). It was evident that the HAMA was in a flow dynamic state (storage modulus G'< loss modulus G'') before light exposure. Once exposed to light, it rapidly formed into a more robust hydrogel with double network structure (Fig. 8B i), suggesting photo and the storage modulus was higher enough ($G' = 4326 \pm 73$ Pa). The compressive modulus was significantly elevated from 30 to 316 kPa (Fig. 8B iii), and also exhibits excellent shear strength (Fig. 8B iv). Two months after surgery, the cornea treated with C3H1 hydrogel still had good transparency and appropriate curvature, and histological characterization also revealed that the C3H1 hydrogel filled corneal stroma underwent highly ordered arrangement and regeneration at the defected site (Fig. 8C). Meanwhile, Ger, T.-Y., *et al.* coating ceria nanoparticles with a natural brown and enhanced the ocular bioavailability of nanotherapeutics for corneal epithelial injury recovery.[72] Huang, J., *et al.* inspired by the corneal epithelial basement membrane, proposed a bioactive hydrogel designed.[73] They found that this hydrogel could significantly accelerate the healing rate of corneal wounds. By four weeks after surgery, HEP@GEL had almost completely helped the cornea repair (Fig. 8D).

In recent decades, highly tunable gel substances have garnered significant attention as potential vitreous substitutes, aiming to replicate the natural vitreous in terms of morphological structure, mechanical function, physiological and biochemical properties, and biocompatibility.[93,94] Specifically, synthetic hydrogel-based vitreous substitutes have emerged as promising candidates due to their desirable attributes, such as high-water content, excellent stability, and controllable viscoelastic and mechanical properties.[95–97] Jin, Y., *et al.* proposed a novel DNA supramolecular hydrogel as a potential artificial vitreous substitute.[74] The integrity of the retina and lens was examined by ultrasound at 1 month and 2 months after surgery (Fig. 8E i, ii). Two dark (hypoechoic) zones were observed, which corresponded to the transparent lens and vitreous body, respectively (labeled by dotted line biconvex and asterisk). Chen, M., *et al.* designed poly (ethylene glycol) hydrogel controls the recurrence of choroidal melanoma and preserve vision after vitrectomy.[75] He, B., *et al.* synthesized polycarboxybetaine macromonomer hydrogel for vitreous substitute.[76] The frequency sweep test was conducted to record storage modulus change of and all the G' values were almost constant, suggesting they maintained a stable hydrogel state even after immersing for 1 month. Cai, Y., *et al.* evaluated two peptide hydrogels and introduced optical coherence tomography for retinal microvascular detection in non-pigmented rabbits.[77] Both two kind of hydrogel (3E-OX and 3K-OX) underwent self-assembly within the 60 min, with G' values of approximately 1.0×10^3 and 1.5×10^2 Pa, respectively. Subsequently, a large strain (1000%) was applied for 1 min to thin the hydrogel 3E-OX, which recovered completely within a few minutes when the applied strain was reduced to 0.2%, indicative of its shear-thin recovery properties. A similar trend was observed in gel 3K-OX.

3.3 Smart sensor

The rheological characteristics of hydrogels significantly influence their fixation capabilities and responsiveness to biomolecules. Hydrogels exhibiting optimal viscoelastic properties are capable of rapidly reacting to external stimuli, such as variations in pressure and temperature, and converting these stimuli into electrical signals, thereby enhancing the sensitivity and stability of biosensors.[98] Hydrogels with favorable rheological properties can adapt to diverse environmental conditions, allowing them to maintain consistent performance, which in turn facilitates stable signal transmission in sensors.[99–101]

Li, M. and his colleagues synthesized a printable intelligent sensor.[78] This sensor was based on PVA/ALG/cellulose nanofibers matrix material cross-linked with sodium tetraborate, named as SPBC. The sensor can be attached to the fingers, wrist, and other parts. The results manifested that different bending angles result in different hydrogel strains and different resistance changes (Fig. 9A i). Meanwhile, the graph of the shear rate of each hydrogel sample is shown in Fig. 9A ii, and the viscosity decreases gradually as the shear rate increases, which means that SPBC hydrogel to be smoothly extruded from the printing needle through the syringe under a certain pressure (Fig. 9A ii). Lim, C., *et al.* developed a transcutaneous oxygen pressure (tcPO2) sensor using an ultrathin functionalized hydrogel.[79] The hydrogel was integrated into a three-electrode electrochemical device contained platinum black nanostructure as the working electrode, a platinum thin film as the counter electrode, and a silver/silver chloride reference electrode (Fig. 9B i). The sensor was encapsulated with a multilayer oxygen barrier film to prevent oxygen exchange with the external environment and to maintain the electrochemical performance of the hydrogel–electrode interface (Fig. 9B ii). This diffused oxygen was electrochemically reduced at the working electrode, allowing the reduction current to be measured and correlated with the oxygen concentration (Fig. 9B iii). The sensor demonstrated reliable performance, with current readings varying with leg position (Fig. 9B iv). Liu, W., *et al.* proposed a hydrogel composed of PVA an electrocardiogram signals detection electrode.[80] The electrodes adhere to the skin when applied hot and are easily and residue-free removed when applied cold (Fig. 9C). Zhao, D., *et al.* synthesized device/skin interface based on an adhesive and hydrophobic bilayer hydrogel.[81] This system is capable of analyzing the results of the electroencephalogram signals, showing the volunteer's emotional classification (positive, neutral, negative) (Fig. 9D).

4. Conclusion and future outlook

Rheology is integral to the application of hydrogels, as it provides insights into their mechanical properties and dynamic behavior. The rheological properties of hydrogels are influenced by various factors, including chemical composition, crosslinking density, degree of swelling, and environmental conditions. Primarily, the chemical structure and crosslinking density are crucial determinants of a hydrogel's rheological properties. By modulating the crosslinking density of polymer

chains, the viscoelastic behavior of hydrogels can be tailored, thereby enhancing their suitability for biomedical applications.[102,103] Moreover, the extent of swelling dictates the water content within the hydrogel, subsequently influencing its flexibility and mechanical strength, both of which are essential considerations in the design of hydrogels for applications such as drug delivery and tissue engineering.[104] Additionally, variations in temperature or other external stimuli can significantly impact the rheological properties of hydrogels, particularly in thermoresponsive variants, which experience phase transitions at specific temperatures, thereby altering their mechanical characteristics.[105] However, current research predominantly focuses on material design, and there is an insufficient understanding of the coupling mechanisms between rheology and critical aspects of clinical translation (such as biocompatibility, degradation kinetics, and scalable manufacturing), which impedes the clinical translation of high-performance rheological hydrogels.

Future research should focus on the coupling mechanisms between rheological behavior and the key challenges of clinical translation (such as biocompatibility, *in vivo* degradation kinetics, and the process adaptability required for scale-up manufacture). Initially, it should systematically investigate the quantitative effects of rheological control parameters (*e.g.*, crosslink density and radical generation) on cellular behavior, and through optimization of photopolymerization kinetics and incorporation of biodegradable crosslinking bonds, reduce cytotoxicity while maintaining target rheological properties, thereby addressing the "rheological performance–biocompatibility" challenge. Besides, developing dynamic rheological monitoring and clinical adaptation technologies. Integrate *in situ* rheological characterization (*e.g.*, optical coherence tomography combined with rheological imaging) with biosensing techniques to track the *in vivo* mechanical evolution of hydrogels in real time, thereby providing data support for personalized therapeutic regimens. Moreover, mimicking the dynamic rheological responses of native tissues (shear thinning in muscle, viscoelastic hysteresis in cartilage, *etc.*), and developing hydrogel systems with adaptive mechanics that actively generate rheological behaviors to enhance mechanical matching with host tissues and reduce post-implantation foreign body reactions.

Author contributions

Conceptualization, W. J. and J. S.; methodology, J. S.; software, W. J. and J. S.; data curation: W. J.; data acquisition: W. J. and J. S.; writing—original draft preparation, W. J. and J. S.; writing—review and editing, W. J. and J. S.; supervision, J. S.; project administration, J. S. All authors have read and agreed to the published version of the manuscript.

Conflicts of interest

There are no conflicts to declare.

Abbreviation

HAMA	Methacrylated hyaluronic acid
pDCSM-G	Porcine decellularized corneal stroma matrix hydrogel
CMC	Carbodiimide metho-*p*-toluene sulfonate
NHS	*N*-Hydroxy succinimide
PEG-PCL	Polyethylene glycol-polycaprolactone
PDA	Polydopamine
MC	Methylcellulose
CHI	Chitosan
PVA	Polyvinyl alcohol
SEB	Solid-state epidermal biomarker
$tcPO_2$	transcutaneous oxygen pressure
ECG	Electrocardiogram
EEG	Electroencephalogram

Data availability

No primary research results, software or code have been included and no new data were generated or analyzed as part of this review.

Acknowledgements

This research did not receive any specific grant from funding agencies in the public, commercial, or not-for-profit sectors. The authors express their gratitude to HOME for Researchers (https://www.home-for-researchers.com/) for providing language polishing services, as well as to Figdraw, PowerPoint and Adobe Illustrate for the assistance in creating and assembling images.

References

1 G. W. Hong, *et al.*, Rheological Characteristics of Hyaluronic Acid Fillers as Viscoelastic Substances, *Polymers*, 2024, **16**(16), 2386.
2 Z. Trivedi, *et al.*, Rheological Analysis and Evaluation of Measurement Techniques for Curing Poly(Methyl Methacrylate) Bone Cement in Vertebroplasty, *ACS Biomater. Sci. Eng.*, 2024, **10**(7), 4575–4586.
3 W. Jiao, *et al.*, Mesoporous silica nanoparticles as sensitizers: A novel approach to enhancing shear wave elastography in liver stiffness measurement, *Biomater. Adv.*, 2025, **169**, 214171.
4 E. L. Reeves, *et al.*, Investigating the contribution of hyaluronan to the breast tumour microenvironment using multiparametric MRI and MR elastography, *Mol. Oncol.*, 2023, **17**(6), 1076–1092.
5 W. T. H. Lim, *et al.*, The role of shear viscosity as a biomarker for improving chronic kidney disease detection using shear wave elastography: A computational study using a validated finite element model, *Ultrasonics*, 2023, **133**, 107046.

6 M. Bercea, Rheology as a Tool for Fine-Tuning the Properties of Printable Bioinspired Gels, *Molecules*, 2023, **28**(6), 2766.
7 T. Yang, *et al.*, Bridging the Hydration Barrier: Hydrogel Adhesives for Oral Hard-Soft Tissue Integration, *Biomacromolecules*, 2026, **27**(2), 1097–1121.
8 H. Gao, *et al.*, Dynamic covalent bonding based polysaccharide hydrogels and their applications in wound dressings: A review, *Colloids Surf., B*, 2025, **254**, 114878.
9 W. Jiao, *et al.*, Study of Several Alginate-Based Hydrogels for *In Vitro* 3D Cell Cultures, *Gels*, 2022, **8**(3), 147.
10 W. Yuan, *et al.*, Ultra-stretchable, self-recoverable, notch-insensitive, self-healable and adhesive hydrogel enabled by synergetic hydrogen and dipole-dipole crosslinking, *Mater. Horiz.*, 2025, **12**(7), 2223–2233.
11 G. Chen, *et al.*, Applications of Hydrogels with Special Physical Properties in Biomedicine, *Polymers*, 2019, **11**(9), 1420.
12 O. Kapusta, *et al.*, Antimicrobial Natural Hydrogels in Biomedicine: Properties, Applications, and Challenges-A Concise Review, *Int. J. Mol. Sci.*, 2023, **24**(3), 2191.
13 L. Nie, *et al.*, Editorial: Biocompatible hydrogels: properties, synthesis and applications in biomedicine, *Front Chem*, 2024, **12**, 1500836.
14 H. J. Lee, *et al.*, Regulation of the Viscoelastic Properties of Hyaluronate-Alginate Hybrid Hydrogel as an Injectable for Chondrocyte Delivery, *ACS Omega*, 2020, **5**(25), 15567–15575.
15 S. Michida, U. I. Chung and T. Katashima, Probing the Molecular Mechanism of Viscoelastic Relaxation in Transient Networks, *Gels*, 2023, **9**(12), 945.
16 O. Chaudhuri, *et al.*, Hydrogels with tunable stress relaxation regulate stem cell fate and activity, *Nat. Mater.*, 2016, **15**(3), 326–334.
17 S. Zhang, *et al.*, Observation of topological hydrogen-bonding domains in physical hydrogel for excellent self-healing and elasticity, *Nat. Commun.*, 2025, **16**(1), 2371.
18 C. Liu, *et al.*, Engineering the viscoelasticity of gelatin methacryloyl (GelMA) hydrogels *via* small "dynamic bridges" to regulate BMSC behaviors for osteochondral regeneration, *Bioact Mater*, 2023, **25**, 445–459.
19 X. Liu, *et al.*, Viscoelastic cues to induce stem cell migration and neuronal differentiation in cell-free hydrogel-assisted TBI recovery, *Chem. Eng. J.*, 2024, **492**, 152401.
20 N. Giruzzi, Plenity (Oral Superabsorbent Hydrogel), *Clin Diabetes*, 2020, **38**(3), 313–314.
21 A. Pass, *et al.*, Oral Superabsorbent Hydrogel (Plenity) for Weight Management, *Ann Pharmacother*, 2021, **55**(9), 1146–1152.
22 V. Y. Ho, G. K. Shah and E. M. Liu, ReSure Sealant for Pars Plana Vitrectomy Wound Closure, *Ophthalmic Surg. Lasers Imaging Retina*, 2015, **46**(10), 1042–1044.
23 F. S. Mah, Effect on Gel Formation Time of Adding Topical Ophthalmic Medications to ReSure Sealant, an *In Situ* Hydrogel, *J. Ocul. Pharmacol. Ther.*, 2016, **32**(6), 396–399.
24 S. Ganguli, *et al.*, A Water-Based Liquid Embolic: Evaluation of its Safety and Efficacy in a Rabbit Kidney Model, *J Vasc Interv Radiol*, 2021, **32**(6), 813–818.
25 C. Jumelle, *et al.*, Development and characterization of a hydrogel-based adhesive patch for sealing open-globe injuries, *Acta Biomater.*, 2022, **137**, 53–63.
26 L. Quan and D. M. Kalyon, Parallel-Disk Viscometry of a Viscoplastic Hydrogel: Yield Stress and Other Parameters of Shear Viscosity and Wall Slip, *Gels*, 2022, **8**(4), 230.
27 A. R. Osi, *et al.*, Three-Dimensional-Printable Thermo/Photo-Cross-Linked Methacrylated Chitosan-Gelatin Hydrogel Composites for Tissue Engineering, *ACS Appl. Mater. Interfaces*, 2021, **13**(19), 22902–22913.
28 T. H. Qazi, V. G. Muir and J. A. Burdick, Methods to Characterize Granular Hydrogel Rheological Properties, Porosity, and Cell Invasion, *ACS Biomater. Sci. Eng.*, 2022, **8**(4), 1427–1442.
29 X. Pan, *et al.*, Nanolignin-Facilitated Robust Hydrogels, *ACS Nano*, 2024, **18**(35), 24095–24104.
30 T. Wang, *et al.*, Intraarticularly injectable silk hydrogel microspheres with enhanced mechanical and structural stability to attenuate osteoarthritis, *Biomaterials*, 2022, **286**, 121611.
31 M. G. Bezold, *et al.*, Shear-thinning hydrogel for allograft cell transplantation and externally controlled transgene expression, *Biomaterials*, 2025, **314**, 122812.
32 S. S. Yengul, P. E. Barbone and B. Madore, Dispersion in Tissue-Mimicking Gels Measured with Shear Wave Elastography and Torsional Vibration Rheometry, *Ultrasound Med Biol*, 2019, **45**(2), 586–604.
33 A. Vinod, *et al.*, Gels That Serve as Mucus Simulants: A Review, *Gels*, 2023, **9**(7), 555.
34 T. Gao, *et al.*, Optimization of gelatin-alginate composite bioink printability using rheological parameters: a systematic approach, *Biofabrication*, 2018, **10**(3), 034106.
35 Z. Yang, *et al.*, Nonlinear Behavior of Gelatin Networks Reveals a Hierarchical Structure, *Biomacromolecules*, 2016, **17**(2), 590–600.
36 B. N. Narasimhan, *et al.*, A comparative study of tough hydrogen bonding dissipating hydrogels made with different network structures, *Nanoscale Adv*, 2021, **3**(10), 2934–2947.
37 S. Fang, *et al.*, Design and evaluation of high-viscosity gelatin/polyacrylamide/sodium alginate triple-network hydrogels for 3D printing: fluid dynamics simulation and experimental method, *Int. J. Biol. Macromol.*, 2025, **318**(Pt 1), 144886.
38 K. Lei, *et al.*, Polysaccharide-based recoverable double-network hydrogel with high strength and self-healing properties, *J. Mater. Chem. B*, 2020, **8**(4), 794–802.
39 J. J. Zhang, *et al.*, Harnessing Mechanical Stress with Viscoelastic Biomaterials for Periodontal Ligament Regeneration, *Adv Sci*, 2024, **11**(18), e2309562.
40 A. K. Nguyen, *et al.*, Hierarchical assembly of tryptophan zipper peptides into stress-relaxing bioactive hydrogels, *Nat. Commun.*, 2023, **14**(1), 6604.

41 G. Vincent, Timescales in creep and yielding of attractive gels, *Soft Matter*, 2014, **10**(10), 1555–1571.
42 F. L. C. Morgan, *et al.*, Tuning Hydrogels by Mixing Dynamic Cross-Linkers: Enabling Cell-Instructive Hydrogels and Advanced Bioinks, *Adv Healthc Mater*, 2022, **11**(1), e2101576.
43 W. Tian, *et al.*, Flexible control of bigel microstructure for enhanced stability and flavor release during oral consumption, *Food Res. Int.*, 2023, **174**(Pt 1), 113606.
44 T. U. Rehman, L. A. Shah and H. Yoo, Molecular topology and rheological study of guar gum and bentonite reinforced polymer hydrogels for potential application in strain sensor and electrode materials, *Int. J. Biol. Macromol.*, 2025, **312**, 144169.
45 A. Kulkarni, *et al.*, Gelation and large thermoresponse of cranberry-based xyloglucan, *Carbohydr. Polym.*, 2024, **339**, 122189.
46 T. B. Goudoulas, *et al.*, Comparative Large Amplitude Oscillatory Shear (LAOS) Study of Ionically and Physically Crosslinked Hydrogels, *Polymers*, 2023, **15**(6), 1558.
47 A. Scutte, *et al.*, Rheological Characterization and 3D Fabrication of Artificial Bacterial Biofilms, *ACS Biomater. Sci. Eng.*, 2025, **11**(6), 3455–3466.
48 B. Fan, *et al.*, Self-Healing Injectable Polymer Hydrogel *via* Dynamic Thiol-Alkynone Double Addition Cross-Links, *ACS Macro Lett.*, 2020, **9**(6), 776–780.
49 S. R. Batool, *et al.*, Chitosan-anthracene hydrogels as controlled stiffening networks, *Int. J. Biol. Macromol.*, 2021, **185**, 165–175.
50 J. D. Dos Santos Carvalho, R. S. Rabelo and M. D. Hubinger, Thermo-rheological properties of chitosan hydrogels with hydroxypropyl methylcellulose and methylcellulose, *Int. J. Biol. Macromol.*, 2022, **209**(Pt A), 367–375.
51 T. U. Rehman, L. A. Shah and H. Yoo, Bio-inspired hydrogels comprising organic and inorganic components association explored as Bingham precursor solution for extending direct ink writing technique in 3D printing, *Int. J. Biol. Macromol.*, 2025, **320**(Pt 3), 146098.
52 H. N. Qiu, *et al.*, Stress Relaxation and Creep Response of Glassy Hydrogels with Dense Physical Associations, *ACS Appl. Mater. Interfaces*, 2025, **17**(6), 9981–9991.
53 M. T. Khan, *et al.*, Development of acrylic acid–agar-based adhesive hydrogel: Influence of tannic acid concentration on adhesion performance, *Int. J. Adhes. Adhes.*, 2025, **142**, 104088.
54 F. Ullah, *et al.*, Fabrication of xanthan gum based polymeric hydrogels: Rheological investigation, toughness, and adhesion optimization, *Int. J. Adhes. Adhes.*, 2025, **138**, 103955.
55 N. Zandi, *et al.*, Nanoengineered shear-thinning and bioprintable hydrogel as a versatile platform for biomedical applications, *Biomaterials*, 2021, **267**, 120476.
56 M. G. Bezold, *et al.*, Hybrid Shear-thinning Hydrogel Integrating Hyaluronic Acid with ROS-Responsive Nanoparticles, *Adv. Funct. Mater.*, 2023, **33**(31), 2213368.
57 C. Loebel, *et al.*, Shear-thinning and self-healing hydrogels as injectable therapeutics and for 3D-printing, *Nat. Protoc.*, 2017, **12**(8), 1521–1541.
58 L. T. Gao, *et al.*, Tough, self-healing and injectable dynamic nanocomposite hydrogel based on gelatin and sodium alginate, *Carbohydr. Polym.*, 2024, **330**, 121812.
59 Z. Li, *et al.*, Self-Healing Hydrogel Bioelectronics, *Adv. Mater.*, 2024, **36**(21), e2306350.
60 C. Cai, *et al.*, Self-Healing Hydrogel Embodied with Macrophage-Regulation and Responsive-Gene-Silencing Properties for Synergistic Prevention of Peritendinous Adhesion, *Adv. Mater.*, 2022, **34**(5), e2106564.
61 M. Sher, *et al.*, Hybrid strengthening of cellulose nanocrystal-based solvent co-cross linked flexible organohydrogels with fast self-healing, diverse adhesive nature, and anti-freezing behavior for advanced human health monitoring, *J. Mater. Chem. B*, 2025, **13**(15), 4612–4629.
62 W. Jiao, *et al.*, GelMA hydrogel: A game-changer in 3D tumor modeling, *Mater. Today Chem.*, 2024, **38**, 102111.
63 M. Salzano de Luna, *et al.*, Light-responsive and self-healing behavior of azobenzene-based supramolecular hydrogels, *J. Colloid Interface Sci.*, 2020, **568**, 16–24.
64 Z. Fan, *et al.*, Rheological insight of polysaccharide/protein based hydrogels in recent food and biomedical fields: A review, *Int. J. Biol. Macromol.*, 2022, **222**(Pt B), 1642–1664.
65 C. Palomino-Durand, *et al.*, Influence of the Soluble-Insoluble Ratios of Cyclodextrins Polymers on the Viscoelastic Properties of Injectable Chitosan-Based Hydrogels for Biomedical Application, *Polymers*, 2019, **11**(2), 214.
66 X. Yan, *et al.*, Advances in enhancing the mechanical properties of hydrogels through multi-strategic approaches based on biopolymer platforms, *Int. J. Biol. Macromol.*, 2024, **272**(Pt 2), 132583.
67 C. Wu, *et al.*, Sustained Endocytosis Inhibition *via* Locally-Injected Drug-Eluting Hydrogel Improves ADCC-Mediated Antibody Therapy in Colorectal Cancer, *Adv Sci*, 2024, e2407239.
68 B. Singh and L. Pal, Sterculia crosslinked PVA and PVA-poly(AAm) hydrogel wound dressings for slow drug delivery: mechanical, mucoadhesive, biocompatible and permeability properties, *J Mech Behav Biomed Mater*, 2012, **9**, 9–21.
69 K. Chen, *et al.*, Adhesive and Injectable Hydrogel Microspheres for Inner Ear Treatment, *Small*, 2022, **18**(36), e2106591.
70 M. Chen, *et al.*, Injectable Gel-PEG hydrogels as promising delivery system for intravitreal PACAP release: Novel therapeutics for unilateral common carotid artery occlusion induced retinal ischemia, *Biomed. Pharmacother.*, 2024, **179**, 117427.
71 X. Shen, *et al.*, Dual-crosslinked regenerative hydrogel for sutureless long-term repair of corneal defect, *Bioact Mater*, 2023, **20**, 434–448.

72 T.-Y. Ger, *et al.*, Alginate-functionalized nanoceria as ion-responsive eye drop formulation to treat corneal abrasion, *Carbohydr. Polym.*, 2025, **352**, 123164.
73 J. Huang, *et al.*, Biologically inspired bioactive hydrogels for scarless corneal repair, *Sci. Adv.*, 2024, **10**(51), eadt1643.
74 Y. Jin, *et al.*, DNA Supramolecular Hydrogel as a Biocompatible Artificial Vitreous Substitute, *Adv. Mater. Interfaces*, 2021, **9**(5), 2101321.
75 M. Chen, *et al.*, An immunotherapeutic artificial vitreous body hydrogel to control choroidal melanoma and preserve vision after vitrectomy, *Sci. Adv.*, 2023, **9**(44), eadh1582.
76 B. He, *et al.*, An in situ-forming polyzwitterion hydrogel: Towards vitreous substitute application, *Bioact Mater*, 2021, **6**(10), 3085–3096.
77 Y. Cai, *et al.*, Injectable self-assembling peptide hydrogel as a promising vitreous substitute, *J Control Release*, 2024, **376**, 402–412.
78 M. Li, *et al.*, A High-Stretching, Rapid-Self-Healing, and Printable Composite Hydrogel Based on Poly(Vinyl Alcohol), Nanocellulose, and Sodium Alginate, *Gels*, 2024, **10**(4), 258.
79 C. Lim, *et al.*, Tissue-like skin-device interface for wearable bioelectronics by using ultrasoft, mass-permeable, and low-impedance hydrogels, *Sci. Adv.*, 2021, **7**(19), eabd3716.
80 W. Liu, *et al.*, A temperature responsive adhesive hydrogel for fabrication of flexible electronic sensors, *npj Flexible Electron.*, 2022, **6**(1), 68.
81 G. Yang, *et al.*, Adhesive and Hydrophobic Bilayer Hydrogel Enabled On-Skin Biosensors for High-Fidelity Classification of Human Emotion, *Adv. Funct. Mater.*, 2022, **32**(29), 2200457.
82 T. C. Ho, *et al.*, Hydrogels: Properties and Applications in Biomedicine, *Molecules*, 2022, **27**(9), 2902.
83 R. K. Mittal, *et al.*, Hydrogel Breakthroughs in Biomedicine: Recent Advances and Implications, *Curr. Pharm. Biotechnol.*, 2024, **25**(11), 1436–1451.
84 A. Salahuddin, *et al.*, Recent advances in chitosan-based smart hydrogel for drug delivery systems, *Int. J. Biol. Macromol.*, 2024, 135803.
85 Y. Chen, *et al.*, Research advances in smart responsive-hydrogel dressings with potential clinical diabetic wound healing properties, *Mil Med Res*, 2023, **10**(1), 37.
86 L. Budai, *et al.*, Rheological Considerations of Pharmaceutical Formulations: Focus on Viscoelasticity, *Gels*, 2023, **9**(6), 469.
87 S. Liu, *et al.*, Gelatin-nanocellulose stabilized emulsion-filled hydrogel beads loaded with curcumin: Preparation, encapsulation and release behavior, *Int. J. Biol. Macromol.*, 2024, **275**(Pt 2), 133551.
88 R. Smith, N. Brogden and J. Fiegel, Sprayable ciprofloxacin-loaded poloxamer hydrogels for wound infection treatment, *J Drug Deliv Sci Technol*, 2023, **89**, 105000.
89 W. Jiao, *et al.*, Construction and Evaluation of Small-Diameter Bioartificial Arteries Based on a Combined-Mold Technology, *Polymers*, 2022, **14**(15), 3089.
90 S. Khosravimelal, *et al.*, Hydrogels as Emerging Materials for Cornea Wound Healing, *Small*, 2021, **17**(30), e2006335.
91 Z. Arabpour, *et al.*, Exploring Hydrogel Nanoparticle Systems for Enhanced Ocular Drug Delivery, *Gels*, 2024, **10**(9), 589.
92 K. Y. Wu, *et al.*, Hydrogels in Ophthalmology: Novel Strategies for Overcoming Therapeutic Challenges, *Materials*, 2023, **17**(1), 86.
93 C. Mondelo-Garcia, *et al.*, Current Situation and Challenges in Vitreous Substitutes, *Macromol. Biosci.*, 2021, **21**(8), e2100066.
94 S. Qu, *et al.*, Desired properties of polymeric hydrogel vitreous substitute, *Biomed Pharmacother*, 2024, **172**, 116154.
95 H. Wang, *et al.*, Antifouling Super Water Absorbent Supramolecular Polymer Hydrogel as an Artificial Vitreous Body, *Adv Sci*, 2018, **5**(11), 1800711.
96 I. Yadav, *et al.*, Vitreous substitutes: An overview of the properties, importance, and development, *J Biomed Mater Res B Appl Biomater*, 2021, **109**(8), 1156–1176.
97 A. Schulz and P. Szurman, Vitreous Substitutes as Drug Release Systems, *Transl. Vis. Sci. Technol.*, 2022, **11**(9), 14.
98 A. Herrmann, R. Haag and U. Schedler, Hydrogels and Their Role in Biosensing Applications, *Adv Healthc Mater*, 2021, **10**(11), e2100062.
99 J. Zhang, *et al.*, Rapid, autonomous high-throughput characterization of hydrogel rheological properties *via* automated sensing and physics-guided machine learning, *Appl. Mater. Today*, 2023, **30**, 101720.
100 A. Miranda-Martinez, *et al.*, Portable Quartz Crystal Resonator Sensor for Characterising the Gelation Kinetics and Viscoelastic Properties of Hydrogels, *Gels*, 2022, **8**(11), 718.
101 B. Ye, *et al.*, Glycopolymer-Based Antiswelling, Conductive, and Underwater Adhesive Hydrogels for Flexible Strain Sensor Application, *ACS Biomater. Sci. Eng.*, 2023, **9**(12), 6891–6901.
102 L. Cacopardo, *et al.*, Engineering hydrogel viscoelasticity, *J Mech Behav Biomed Mater*, 2019, **89**, 162–167.
103 P. Lu, *et al.*, Harnessing the potential of hydrogels for advanced therapeutic applications: current achievements and future directions, *Signal Transduct Target Ther*, 2024, **9**(1), 166.
104 J. Fu and M. In Het Panhuis, Hydrogel properties and applications, *J. Mater. Chem. B*, 2019, **7**(10), 1523–1525.
105 F. Xin and Q. Lyu, A Review on Thermal Properties of Hydrogels for Electronic Devices Applications, *Gels*, 2022, **9**(1), 7.